

# The increasing of charge carriers concentration in thin bismuth films

© E.V. Demidov, V.M. Grabov, V.A. Komarov, A.V. Suslov, V.A. Gerega, A.N. Krushelnitskii

Herzen State Pedagogical University of Russia,  
191186 St. Petersburg, Russia

E-mail: demidov\_evg@mail.ru

Received September 19, 2021

Revised September 24, 2021

Accepted September 24, 2021

The reasons for increasing the charge carriers concentration in thin bismuth films are discussed. The concentration was calculated on the basis of the measured electrical and galvanomagnetic coefficients at the temperature 77 K under the two-band approximation and the assumption that the charge carriers free path in the plane of the film is isotropic.

**Keywords:** Bismuth, thin film, charge carriers concentration, surface.

DOI: 10.21883/SC.2022.02.53118.19

## 1. Introduction

The increased interest in reduced dimension systems is observed for more than 50 years. A special place in these studies is occupied by semimetals and narrow-gap semiconductors, i.e. materials with unprecedented values of the de Broglie wavelength of charge carriers, which characterizes the possibility of observing the quantum effects in solids.

A typical and most studied representative of this class of materials is bismuth, in which a number of coherent effects was theoretically predicted and experimentally observed over the past decades. However, not all theoretical predictions in this area were reliably confirmed by experiments.

The papers [1–3] theoretically predicted that due to the quantum size effect a semimetal–semiconductor transition should be observed in bismuth crystals at sample sizes of the order of the de Broglie wavelength of charge carriers.

Over the past few decades, repeated attempts have been made to experimentally establish the semimetal–semiconductor transition in thin bismuth films and filaments [4–6]. However, despite the significant efforts in this direction, the experimental results and their interpretation remain ambiguous. For example, the papers [7,8] report not decreasing, but increasing of the concentration of charge carriers with the thickness decreasing of the bismuth films.

In this paper, an attempt was made to establish the causes of this contradiction in the information about the properties of thin bismuth films.

## 2. Experimental procedure

Bismuth films were obtained by thermal evaporation in vacuum. Bismuth with a purity of 99.999% was used for evaporation. Mica (muscovite) grade SOV (plate thickness 0.005–0.04 mm) was used as a substrate.

To obtain films with a thickness of 150 nm and less the electron-beam evaporation in vacuum of  $\sim 10^{-6}$  Pa at the bismuth deposition rate of 0.1 nm/s was used. For films

300 nm thick the thermal evaporation in vacuum  $\sim 10^{-3}$  Pa was used at the bismuth deposition rate of 5 nm/s. Films 150 nm thick and less were obtained at the substrate temperature of 413 K and an annealing temperature of 473 K, the annealing time was 1 h. Films 300 nm thick were obtained at various substrate temperatures from 353 to 473 K with and without annealing; the annealing time was 30 min. To obtain a single-crystal film of this thickness, zone recrystallization under a protective coating was used [9]. If annealing was used, the obtained films were annealed without the vacuum braking just after the film formation.

The thickness of films 150 nm thick and less was checked by atomic force microscopy in a contact mode according to a specially developed procedure, using selective chemical etching of crystal boundaries [10]. The thickness of films 300 nm thick was checked on a Linnik interferometer. The error of the film thickness determination by these methods did not exceed 10%.

The crystal structure of the films was checked using a „DRON-7“ X-ray diffractometer („Burevestnik“ company).

The crystal sizes were determined on Solver-P47 Pro scanning probe microscope of NT-MDT Company using selective chemical etching [11] or decoration using natural oxidation [12]. The size of crystals is determined with an accuracy of  $\sim 10\%$ .

To study the electrical properties of bismuth films, the contact pads made of copper or manganin were formed by thermal spraying.

The study of electrical and galvanomagnetic properties (resistivity, magnetoresistance, Hall coefficient) was carried out according to the classical procedure at direct current and constant magnetic field at temperature of 77 K.

Measurement error of resistivity and Hall coefficient is 10%. The relative magnetoresistance was measured with the error of 5%.

The scientific equipment of the Shared-Access Interdisciplinary Resource Center „State of art physical and chemical methods for the formation and study of materials for

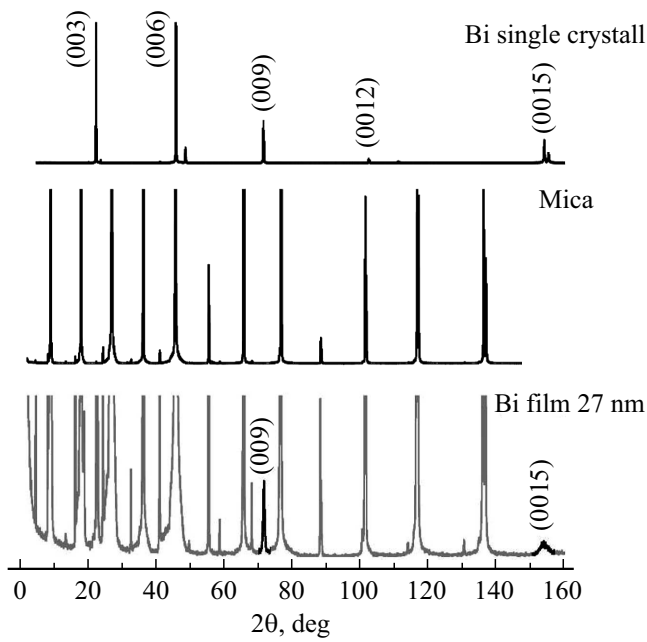


**Figure 1.** X-ray diffraction patterns of single crystal of bismuth, of mica and of bismuth film.

the needs of industry, science and education“ (Herzen University) was used in the paper.

### 3. Experimental results and discussion

#### 3.1. Structure of thin films

The structure study of the obtained films by X-ray diffraction analysis showed that bismuth films > 25 nm thick have a crystallographic orientation corresponding to the orientation of (111) plane parallel to the substrate plane. The position of the diffraction maxima in the diffraction patterns of the bismuth films coincides with the position of the maxima of (111) plane of the bismuth single crystal. This indicates the equality of the interplanar distances in the bismuth film and the bismuth single crystal.

As an example, Fig. 1 shows diffraction patterns obtained by  $\theta - 2\theta$  scheme for the bismuth film 27 nm thick on mica, for mica and for bismuth single crystal. The maxima belonging to bismuth are noted. The positions of the maxima of the bismuth film crystal and the single crystal completely coincide. In this paper good diffraction patterns were not obtained for bismuth films < 25 nm thick. Perhaps this is due to the low signal-to-noise ratio or to the structure modification of the films with such thicknesses.

In the paper [11] it was shown that there are hillocks on the surface of bismuth films on mica substrate obtained by vacuum thermal evaporation. The concentration of these formations rapidly decreases with the substrate temperature increasing during the films formation [13]. In this paper, the atomic force microscopy also revealed these structures in bismuth films. The block sizes were determined taking into

account the concentration and size of hillocks according to the method described in the papers [14,15].

#### 3.2. Method for determining the concentration of charge carriers in bismuth films

The main sign of the bismuth transition from semimetallic state to semiconductor with the film thickness decreasing is the concentration decreasing of the charge carriers. The concentration of charge carriers in bismuth films was determined based on the measured transfer coefficients: resistivity ( $\rho$ ), Hall coefficient ( $R$ ), and magnetoresistance ( $\frac{\Delta\rho}{\rho B^2}$ ) in weak magnetic field.

The calculation was carried out within the boundaries of the two-band approximation, assuming equal concentrations of electrons and holes, and weak magnetic field. In this approximation, taking into account the crystallographic orientation of the films, the resistivity, magnetoresistance, and Hall coefficient measured in them correspond to the components of the tensors of the galvanomagnetic coefficients of bismuth single crystal  $\rho_{11}$ ,  $\rho_{11,33}$ ,  $R_{12,3}$ . The indices indicate the designation of the axes in the crystallographic coordinate system (axis 1 is parallel to the symmetry axis of the crystal  $C_2$ , axis 3 is parallel to the symmetry axis  $C_3$ , and the axis 2 is perpendicular to  $C_2$  and  $C_3$ ). The transfer coefficients  $\rho_{11}$ ,  $\rho_{11,33}$ ,  $R_{12,3}$  in the weak transverse magnetic field are usually expressed in terms of elementary charge  $e$ , concentration  $n$  and mobility components of the charge carriers in coordinate systems related to the symmetry axes of electron and hole ellipsoids  $u_1^-, u_2^-, u_1^+ = u_2^- = u^+$ :

$$\sigma = \frac{1}{\rho} = \sigma_{11} = -en \left[ \frac{1}{2}(u_1^- + u_2^-) + u^+ \right], \quad (1)$$

$$R = R_{12,3} = \frac{en}{\sigma_{11}^2} [u_1^- u_2^- - (u^+)^2], \quad (2)$$

$$\frac{\Delta\rho}{B^2} = \rho_{11,33} = -\rho_{11}^2 \left[ enu^{+3} + \frac{1}{2} enu_1^- u_2^- (u_1^- + u_2^-) \right] - \sigma_{11} (R_{12,3})^2. \quad (3)$$

In the analysis of the transfer phenomena in highly perfect bulk crystals of bismuth, the relaxation time isotropy approximation is often used. In samples with high defects content, the isotropy approximation of the mean free path [16,17] is more applicable, therefore, in the case of films with thicknesses much less than the mean free path of electrons in the bulk crystal it is possible to use the isotropy approximation of the electron mean free path ( $L$ ) in plane of the substrate ( $L_1 = L_2$ ).

Let us estimate the mean free path of electrons in bismuth in plane (111) at temperature of 77 K in the bulk single crystal, i.e. due to scattering on phonons:

$$L = \frac{1}{|e|} u \sqrt{2E_F m^*}, \quad (4)$$

where  $u$  is mobility,  $E_F$  is Fermi energy,  $m^*$  is effective mass.

The Fermi energy and components of the mobility tensor and effective masses of electrons along the principal axes of the Fermi surface of the bismuth single crystal at temperature of 77 K

Axis	$u$ , $\text{m}^2/\text{V} \cdot \text{s}$	$E_F$ , meV	$m^*$	$L$ , $\mu\text{m}$
1	85.19	14.4	$0.006 \cdot m_0$	1.90
2	4.19	14.4	$1.27 \cdot m_0$	1.35

Note.  $m_0$  is free electron mass.

The calculation used data from the paper [18] for temperature of 77 K, presented in the Table.

The calculation results are presented in the last column of the Table.

Thus, the mean free paths of electrons in bismuth in the plane (111), due to scattering on phonons at temperature of 77 K, are  $> 1 \mu\text{m}$ ; therefore, in the case of predominantly diffuse scattering of charge carriers by the surface, even for films 300 nm thick the isotropy approximation of the mean free path can be used.

In this case, for  $L_1 = L_2$  film and, respectively, for the bismuth film

$$\frac{u_1^-}{u_2^-} = \sqrt{\frac{m_2^*}{m_1^*}} \approx 14.5. \quad (5)$$

Thus, using the numerical solution of the system of equations 1–3 and 6, using the values of the measured transfer coefficients, the concentrations and mobilities in the obtained bismuth films were calculated.

As in the paper the sufficiently thin films are used, in which size quantization is implemented, and the role of the surface electronic structure increases, the approximation of the equality of the concentrations of electrons and holes can be violated. In this regard, we will use this approximation as a hypothesis, while evaluating the possibility of its application on the basis of the results obtained.

### 3.3. Effect of block sizes on the concentration and mobility of charge carriers in bismuth films

In some papers, it is reported that the reason for the concentration increasing of charge carriers in thin films of bismuth may be the additional concentration due to the presence of free surface [4,19,20]. This is a reasonable assumption, since this situation is quite common in semiconductors. Since bismuth films are in most cases are block-structured, the additional concentration of charge carriers can also be formed due to the presence of crystal boundaries.

Then the concentration in the film will be determined by the expression:

$$n_{\text{film}} = n_{\text{bulk}} + n_{\text{surface}} \cdot d_{\text{surface}} \cdot \frac{1}{h} + n_{\text{crystal boundary}} \cdot d_{\text{crystal boundary}} \cdot \frac{1}{G}, \quad (6)$$

where  $n_{\text{bulk}}$  is concentration in the bulk single crystal of bismuth,  $n_{\text{surface}}$  is additional concentration of charge carriers due to the presence of free surface,  $d_{\text{surface}}$  is thickness of the surface layer in which the additional concentration of charge carriers is formed,  $n_{\text{crystal boundary}}$  is additional concentration of charge carriers due to the presence of crystal boundaries,  $d_{\text{crystal boundary}}$  is thickness of crystal boundaries in which the additional concentration of charge carriers is formed,  $h$  is film thickness,  $G$  is crystal size.

Thus, if the additional concentration of charge carriers is formed at the crystal boundaries in bismuth film for films of fixed thickness, but having different crystal sizes, its values will be linearized in the coordinates  $n_{\text{film}}$  from  $1/G$ , and the gradient of the straight line will be equal to  $n_{\text{crystal boundary}} \cdot d_{\text{crystal boundary}}$ . The similar situation will also occur in the case of the fixed crystal size for films with variable thickness. In this case, the values of charge carrier concentration will be linearized in the coordinates  $n_{\text{film}}$  from  $1/h$ .

By analogy with expression (6), in the case of independence of the contributions of various scattering mechanisms to the limitation of charge carrier mobilities by phonons ( $1/u_{\text{phon}}$ ), surface ( $1/u_h$ ), and crystal boundaries ( $1/u_G$ ), in accordance with the Matthiessen rule we can write

$$\frac{1}{u_{\text{film}}} = \frac{1}{u_{\text{phonons}}} + a \cdot \frac{1}{h} + b \cdot \frac{1}{G}, \quad (7)$$

where  $u$  is  $u_1^-$ ,  $u_2^-$  or  $u^+$ ,  $a$  is coefficient characterizing scattering of charge carriers by the surface,  $b$  is coefficient characterizing the scattering of charge carriers by crystal boundaries.

The linear form of the of the mobility value dependences in coordinates  $1/u$  from  $1/G$  or  $1/h$  in the case of fixed thickness or sizes of crystals can be a validity criterion of the used approximations, including the assumption that the concentrations of electrons and holes are equal.

It is technologically much easier to produce a series of films with fixed thickness and variable crystal size as compared to the series of films with fixed crystal size and variable thickness. In this connection, for the experimental verification of expression (7) a series of bismuth films 300 nm thick with crystal sizes from 0.9 to 6.3  $\mu\text{m}$ , as well as single-crystal film obtained by zone recrystallization under a coating were obtained. Films with different crystal sizes were obtained using various substrate temperatures in the range from 353 to 473 K, and the presence or absence of annealing during film formation. In the obtained films the resistivity, magnetoresistance, and Hall coefficient were measured in weak magnetic fields, and the concentrations and mobility of charge carriers were calculated. In all expressions reflecting the obtained linear dependences of the concentration and mobility of charge carriers, the use of the international system of units SI is implied.

Fig. 2 shows the mobility of electrons and holes in the coordinates  $1/u$  vs.  $1/G$ . As in earlier papers, for example [14], and considering a small statistical scattering,

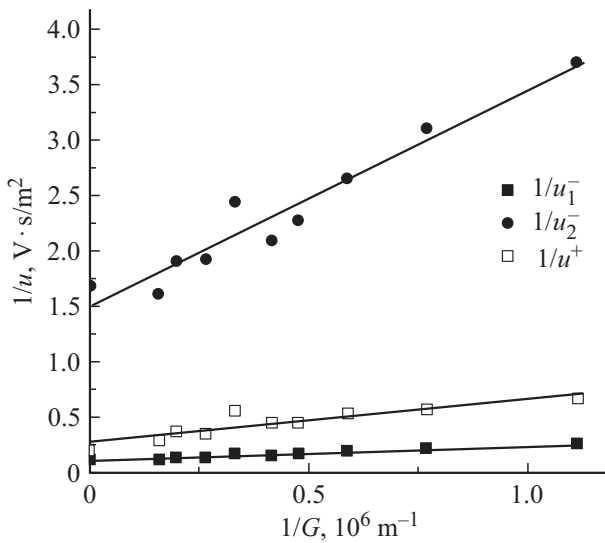


**Figure 2.** Inverse values of mobility of electrons and holes vs.  $1/G$  for bismuth films 300 nm thick at temperature of 77 K.

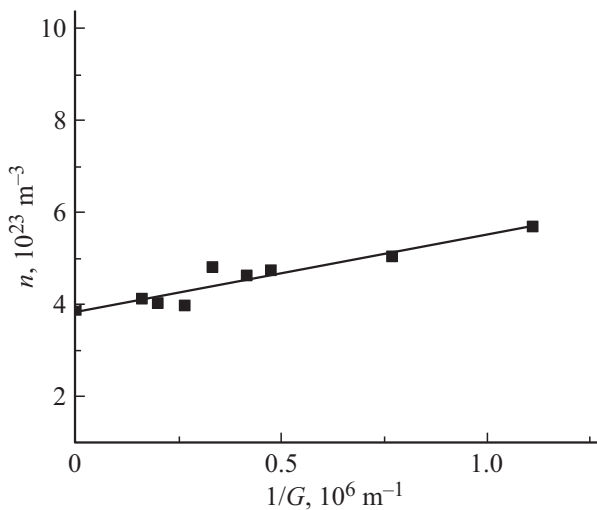


**Figure 3.** Charge carriers concentration vs.  $1/G$  for bismuth films 300 nm thick at temperature of 77 K.

these dependences are well linearized, which indicates the validity of the assumptions used for the calculation, including the assumption of equality of charge carrier concentrations for films 300 nm thick.

The equations of the approximating straight lines presented in Fig. 2 have the following form:

$$\frac{1}{u_1^-} = 0.1 + 1.36 \cdot 10^{-7} \frac{1}{G}, \quad (8)$$

$$\frac{1}{u_2^-} = 1.49 + 1.97 \cdot 10^{-6} \frac{1}{G}, \quad (9)$$

$$\frac{1}{u^+} = 0.27 + 3.86 \cdot 10^{-7} \frac{1}{G}. \quad (10)$$

Fig. 3 shows the concentration of charge carriers in coordinates  $n$  vs.  $1/G$ . The statistical scattering of the

concentration values is more pronounced than the same of the mobilities. Despite this, the concentration increasing of charge carriers with the decreasing of the crystal size is clearly observed. The equation of the approximating straight line presented in Fig. 3 has the following form:

$$n_{\text{film}} = 3.8 \cdot 10^{23} + 1.7 \cdot 10^{17} \frac{1}{G}. \quad (11)$$

Comparing expressions (6) and (11), we have  $n_{\text{crystal boundary}} \cdot d_{\text{crystal boundary}} = 1.7 \cdot 10^{17} \text{ m}^{-2}$ , standard error is  $0.2 \cdot 10^{17} \text{ m}^{-2}$ .

### 3.4. Effect of film thickness on the concentration and mobility of charge carriers in bismuth films

To determine the surface effect on the concentration of charge carriers in bismuth films the series of bismuth films with thickness of 15 to 300 nm was obtained. The mobilities and concentrations of charge carriers are calculated based on the measured transfer coefficients. We also used data on the mobility and concentration of charge carriers in bismuth single crystal from the paper [18], taking into account the concentration decreasing of carriers in bismuth due to its mechanical deformation as the result of the mismatch between the thermal expansion coefficient of bismuth and mica [21].

Fig. 4 shows the mobility of electrons and holes in the coordinates  $1/u$  vs.  $1/h$  due to scattering by phonons and surface. Scattering due to block boundaries was excluded from the mobilities using the coefficients  $b$  obtained in the previous Section and the measured crystal sizes in the films.

The dependences obtained for electrons in the middle of the studied thickness range clearly show the inverse mobilities decreasing relative to the linear dependence typical for thicker films, which is due to the occurrence of the quantum size effect [22], which leads to the Fermi energy increasing [23] and, accordingly, to the decreasing of inverse mobility of electrons. In films  $< 25$  nm thick the values of the inverse mobilities for electrons and holes are somewhat higher compared to the indicated linear dependence. The reasons for this will be discussed after the analysis of the charge carriers concentration.

The equations of the approximating straight lines presented in Fig. 4 have the following form:

$$\frac{1}{u_1^-} = 1.17 \cdot 10^{-2} + 4.09 \cdot 10^{-8} \frac{1}{h}, \quad (12)$$

$$\frac{1}{u_2^-} = 0.24 + 5.91 \cdot 10^{-7} \frac{1}{h}, \quad (13)$$

$$\frac{1}{u^+} = 7.47 \cdot 10^{-2} + 7.28 \cdot 10^{-8} \frac{1}{h}. \quad (14)$$

Fig. 5 shows the concentration of charge carriers in coordinates vs. inverse thickness of film. Since the films had different crystal sizes in the range of 0.4 to  $6.3 \mu\text{m}$ , for

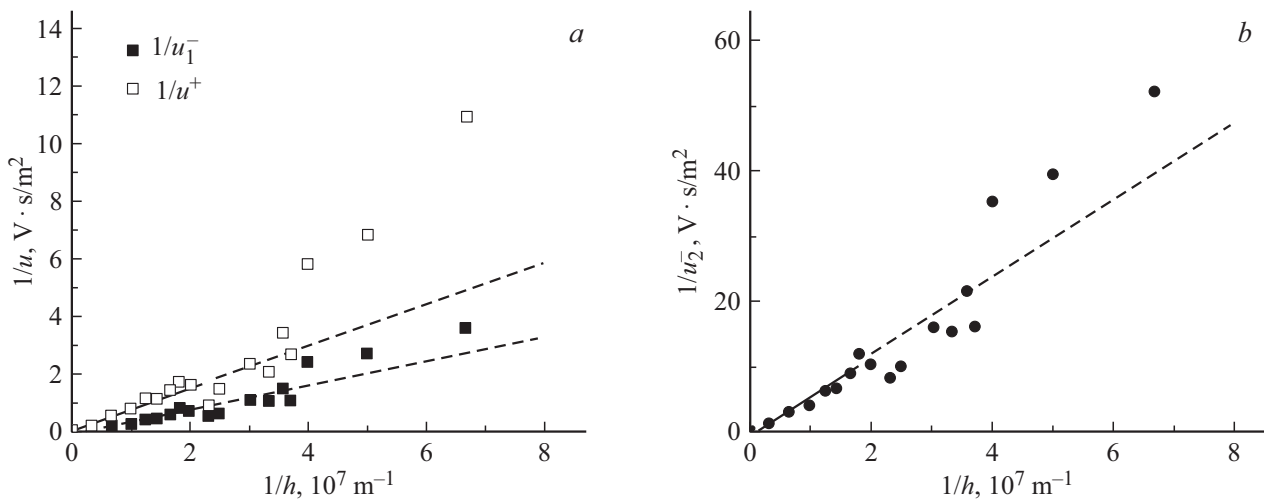


**Figure 4.** Inverse values of mobility of electrons and holes vs.  $1/h$ , due to scattering by phonons and the surface at temperature of 77 K.

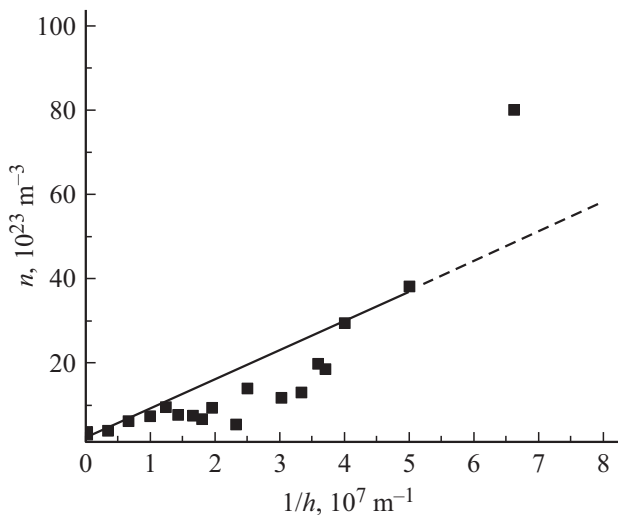


**Figure 5.** Charge carrier concentration vs.  $1/h$  for bismuth films at temperature of 77 K without additional concentration of charge carriers due to the block structure of films.

the experimental data analysis in accordance with expression (6) from the values of charge carrier concentrations, calculated on the basis of the measured transfer coefficients, the concentrations of charge carriers due to the block structure of film were excluded in accordance with the value  $n_{\text{crystal boundary}} \cdot d_{\text{crystal boundary}}$  obtained in the previous Section and the actual size of crystals in the film.

Significant increasing of the charge carriers concentration is observed with the films thickness decreasing. In the section corresponding to films  $> 60$  nm thick the expression (6) is well satisfied. Further, as in the case of electrons mobility, in the middle of the studied thickness range the decreasing of the charge carriers concentration relative to the linear dependence typical for thicker films is clearly observed, but the concentration values for thinner films,

except for film 15 nm thick, return to this straight line, as opposed to electrons mobility.

The concentration decreasing of charge carriers in the middle of the thickness range is due to the occurrence of the quantum size effect, which leads to the concentration decreasing of charge carriers in semimetal films [2,23]. For films 25 nm thick and less, the film goes into „ultraquantum region“ with a possible change in the electronic energy spectrum of charge carriers.

The equation of the approximating straight line shown in Fig. 5 has the following form:

$$n_{\text{film}} = 3 \cdot 10^{23} + 0.7 \cdot 10^{17} \frac{1}{h}. \quad (15)$$

Comparing expressions (6) and (15), we have  $n_{\text{surface}} \cdot d_{\text{surface}} = 0.7 \cdot 10^{17} \text{ m}^{-2}$ , the standard error is:  $0.02 \cdot 10^{17} \text{ m}^{-2}$ .

The concentration of charge carriers in the film 15 nm thick is significantly higher as compared to the linear dependence  $n(1/h)$  obtained for thicker films, which is probably due to the existence of other mechanisms, than those discussed in this article, that ensure the increasing of charge carriers concentration.

Let us return to the issue of low mobility of the charge carriers for films 15–25 nm thick (Fig. 4).

For bismuth it is known that in the case of scattering on phonons the mobility of charge carriers decreases proportionally to their concentration increasing [18]. At the same time, this pattern persists with the concentration increasing, both due to the temperature increasing, and due to doping. It can be assumed that the concentration increasing due to the effect of the surface and boundaries of crystals will also lead to the mobility decreasing of charge carriers. However, the observed concentration increasing of charge carriers in these films and the mobility of electrons and holes upon their scattering on phonons in the bulk single crystal at 77 K do not give such low mobility values

observed in this paper for films 25–15 nm thick. This is probably due to the violation of the assumption that the concentrations of electrons and holes are equal for bismuth films < 25 nm thick. The low values of charge carrier mobilities can also be due to the formation of less perfect crystal boundaries as compared to thicker films. However, studies of the film structure did not reveal any differences in the structure of crystal boundaries for films with thicknesses less and above 251 nm.

#### 4. Conclusion

In this paper in bismuth films with thicknesses equal to about the de Broglie wavelength and much less its values, the semimetal–semiconductor transition was not observed in electrical and galvanomagnetic phenomena. The opposite situation was observed, i.e. the concentration increasing of charge carriers with the film thickness decreasing. The analysis of the obtained experimental results indicates that the reason for the concentration increasing of charge carriers in bismuth films with thickness decreasing is the additional concentration due to the presence of free surface and crystal boundaries. In this case, the quantum size effect reduces the charge carriers concentration. For bismuth films < 25 nm thick, the significant increasing of the charge carriers concentration, possibly, is carried out with breaching of the equality of the concentrations of electrons and holes.

#### Funding

The study was performed under the national task with financial support of Ministry of Education of Russia (project FSN-2020-0026).

#### Conflict of interest

The authors declare that they have no conflict of interest.

#### References

- [1] V.N. Lutsky. *Pis'ma ZhETF*, **2**, 391 (1995) (in Russian).
- [2] V.B. Sandomirsky. *ZhETF*, **52**, 158 (1967) (in Russian).
- [3] Y.-M. Lin, X. Sun, M.S. Dresselhaus. *Phys. Rev. B*, **62**, 4610 (2000).
- [4] P. Hofmann. *Progr. Surf. Sci.*, **81**, 191 (2006).
- [5] V.P. Duggal, R. Rup. *J. Appl. Phys.*, **40**, 492 (1969).
- [6] C.A. Hoffman, J.R. Meyer, F.J. Bartoli, A. Di Venere, X.J. Yi, C.L. Hou, H.C. Wang, J.B. Ketterson, G.K. Wong. *Phys. Rev. B*, **48**, 11431 (1993).
- [7] E.V. Demidov, V.M. Grabov, V.A. Komarov, N.S. Kablukova, A.N. Krushelnitsky. *FTT*, **60**, 452 (2018) (in Russian).
- [8] Yu.F. Komnik, E.I. Bukhshtab, Yu.V. Nikitin, V.V. Andrievsky. *ZhETF*, **60**, 669 (1971) (in Russian).
- [9] V.M. Grabov, V.A. Komarov, N.S. Kablukova, E.V. Demidov, A.N. Krushelnitsky. *Pis'ma ZhETF*, **41**, 20 (2015) (in Russian).
- [10] E.V. Demidov, V.A. Komarov, A.N. Krushelnitsky, A.V. Suslov. *FTP*, **51**, 877 (2017) (in Russian).
- [11] V.M. Grabov, E.V. Demidov, V.A. Komarov. *FTT*, **50**, 1312 (2008) (in Russian).
- [12] V.M. Grabov, E.V. Demidov, V.A. Komarov, M.M. Klimantov. *FTT*, **51**, 800 (2009) (in Russian).
- [13] V.M. Grabov, E.V. Demidov, V.A. Komarov, M.M. Klimantov, D.Yu. Matveev, S.V. Slepnev, E.V. Usynin, E.E. Khristich, E.V. Konstantinov. *Izv. Ross. gos. ped. un-ta im. A.I. Gertsena*, № **95**, 105 (2009) (in Russian).
- [14] V.M. Grabov, E.V. Demidov, V.A. Komarov. *Poverkhnost'. Rentgenovskie, sinhrotronnye i nejtronnye issledovaniya* № **2**, 81 (2011) (in Russian).
- [15] V.M. Grabov, E.V. Demidov, V.A. Komarov. *FTT*, **52**, 1219 (2010) (in Russian).
- [16] J. Zajman. *Electrony i fonony* (M., IIL, 1962).
- [17] F.D. Blatt. *Teoriya podvzhnisti elektronov v tverdykh telakh* (M., Fizmatlit, 1963) (in Russian).
- [18] V.M. Grabov. *Dokt. dis.* (SPb. RGPU im. A.I. Gertsena, 1998) (in Russian).
- [19] T. Hirahara, T. Nagao, I. Matsuda, G. Bihlmayer, E.V. Chulkov, Y.M. Koroteev, P.M. Echenique, M. Saito, S. Hasegawa. *Phys. Rev. Lett.*, **97**, 146803 (2006).
- [20] T. Hirahara, I. Matsuda, S. Yamazaki, N. Miyata, S. Hasegawa, T. Nagao. *Appl. Phys. Lett.*, **91**, 202106 (2007).
- [21] V.M. Grabov, V.A. Komarov, N.S. Kablukova. *FTT*, **58**, 605 (2016) (in Russian).
- [22] E.V. Demidov, V.M. Grabov, V.A. Komarov, A.N. Krushelnitsky, A.V. Suslov, M.V. Suslov. *FTP*, **53**, 736 (2019) (in Russian).
- [23] Yu.F. Komnik. *Fizika metallicheskih plenok* (M., Atomizdat, 1979) (in Russian).